

Supporting Information

*Ruo Chen Xie, Christopher Batchelor-McAuley, Neil P Young and Richard G Compton**

* Corresponding author: Richard G. Compton. Department of Chemistry, Physical & Theoretical Chemistry Laboratory, Oxford University, South Parks Road, Oxford, OX1 3QZ, United Kingdom

Email: richard.compton@chem.ox.ac.uk. Tel: +44(0)1865275 957 Fax: +44(0)1865275410

Contents

S1 – Uncertainty quantification of defining the particle boundary in TEM sizing

S2 – Concentration scaling for the DLS sizing

S2 – Effect of windowing and weighting on the nano-impact sizing results

S1 – Uncertainty quantification of defining the particle boundary in TEM sizing

Limited resolution of TEM images leads to uncertainty in defining a particle's boundary leading to associated errors. This can be quantified by error function fitting on the intensity profile of the images. Specifically, the intensity profile as a function of distance was shown in Figure S1a, along the straight, yellow line drawn across a chosen '20 nm' particle in an image with a pixel size of 0.148 nm (corresponding to a magnification of 150 kx) as an example. One steep drop and then a sharp rise in the intensity curve at the particle boundaries were observed. Next, in the OriginPro 2017, a normal cumulative distribution function as described below was used as the error function and to fit the steep changes (the red curve).

$$y = y_0 + A \int_{-\infty}^x \frac{1}{\sqrt{2\pi} w} e^{-\frac{(t-x_c)^2}{2w^2}} dt$$

where y_0 is the offset in y direction, A is the amplitude of the curve, and x_c is the mean value and w is the standard deviation (STD).

As illustrated in the Origin software, the standard deviation w is associated with the steepness of the amplitude change of the intensity curve as an equation is given that the inter-quarter range IQR

in x axis, $IQR_x = 1.349 w$, so the slope $\approx \frac{IQR_y}{IQR_x} = \frac{0.5 A}{1.349 w}$, and thus $w \propto \frac{1}{\text{slope}}$. This is consistent with the

concept that the steeper the change, the less the uncertainty it has for defining a particle's boundary. As a result, the STDs for the left drop and the right rise in Figure S1a were 0.131 ± 0.099 nm and 0.091 ± 0.107 nm respectively, corresponding to one pixel size or so. Furthermore, to obtain a statistic measure of the uncertainty for a fixed pixel size, 9 boundaries in total across a particle were analysed in the same way and the average were determined as the final uncertainty for this pixel size. As seen from the Figure S1b, the standard deviation ascends with increasing pixel size or decrease in image definition. For the '20 nm' silver particles, such measurement uncertainty

was analysed for the TEM images of all the three pixel sizes 0.148 nm, 0.108 nm and 0.073 nm. As such, the mean STD was determined as 0.139 ± 0.028 nm, corresponding to 1.5 % error in diameter. Likewise, for the '30 nm' particles the 1D measurement uncertainty was found to be 1.6 %.

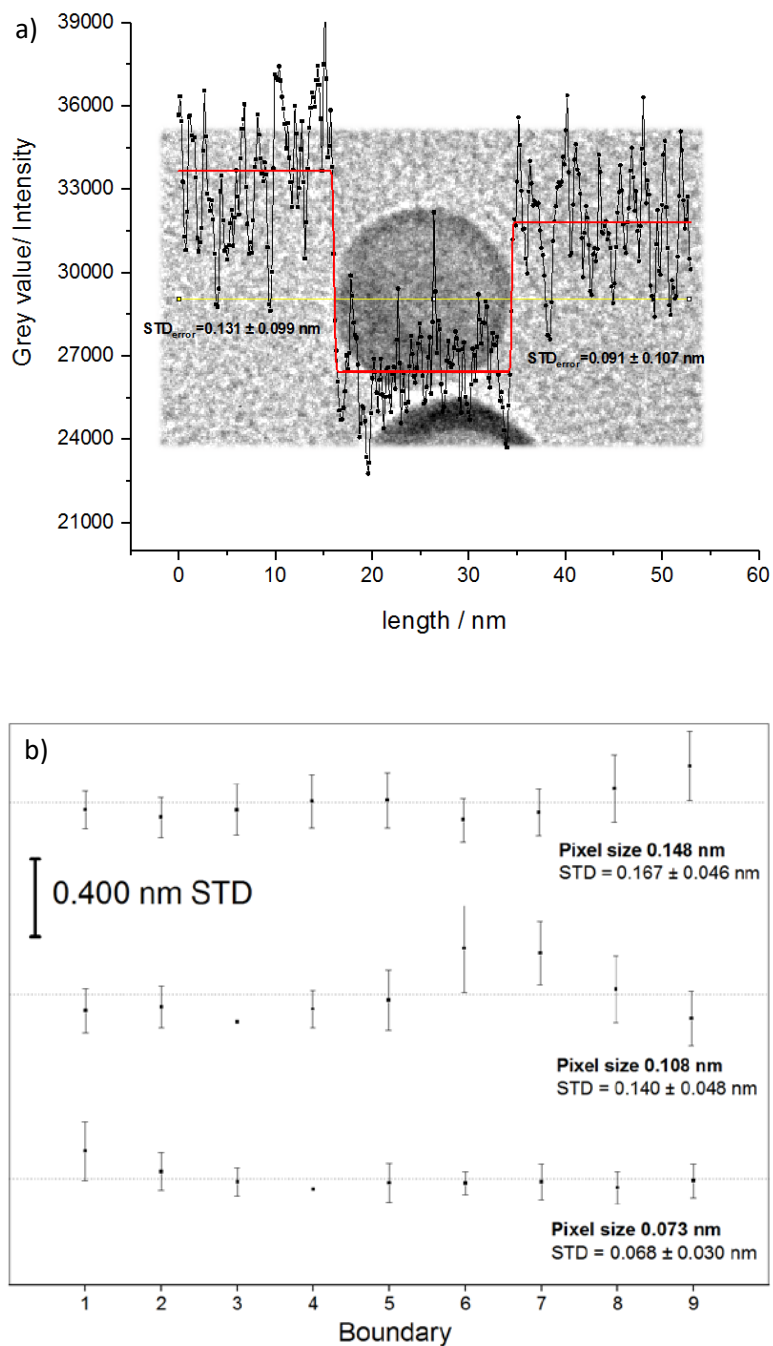


Figure S1. a) Representative superimposed TEM image of one '20 nm' silver particle with the intensity profile (black scatter + line) analysis along the yellow line. The red line represents the error function fitting, giving the standard deviation of defining the boundary position. b) Error analysis upon the TEM sizing for the images with different pixel sizes (0.148 nm, 0.108 nm and 0.073 nm).

S2 – Concentration scaling for the DLS sizing

Several studies have shown that for the DLS measurements of nanoparticles of a small size (e.g. 10 ~ 20 nm in diameter), a high particle concentration such as of the order of nanomolar (nM) may be essential for obtaining an accurate diameter distribution.^{1, 2} As such, the stock dispersion with a concentration of as-synthesised 4.8 nM and the 2, 6, 10, 40, 100, 200, 400, 800-fold diluted dispersions were sized. Accordingly the Z-average diameters were recorded as shown in Fig S2. The figure shows an average mean diameter of 30.5 ± 1.5 nm from 12 pM to 2.4 nM, whereas *ca.* 10 nm higher measured diameters were observed for the 6 pM and the 4.8 nM samples. The latter may be explained that in the 6 pM dispersion the light scattered is so weak that the resulting low count rates of around 150 kcps (or thousand counts per second) and G1 correlation function intercepts of < 0.8 failed to interpret out a meaningful Z-average diameter, while the dense particles in the 4.8 nM dispersion probably results in multiple scattering that biases the results. Therefore, the experimentally measured diameters for the '20 nm' silver particles by DLS are confirmed as *ca.* 30 nm. Similarly, the average diameter of the nominally '30 nm' silver particles was determined as 34.5 ± 0.3 nm from two particle concentrations, 24 pM and as-received 216 pM. Consequently, it is shown that likely improvements in the measurement accuracy with a higher particle concentration does not apply to our silver nano-systems.

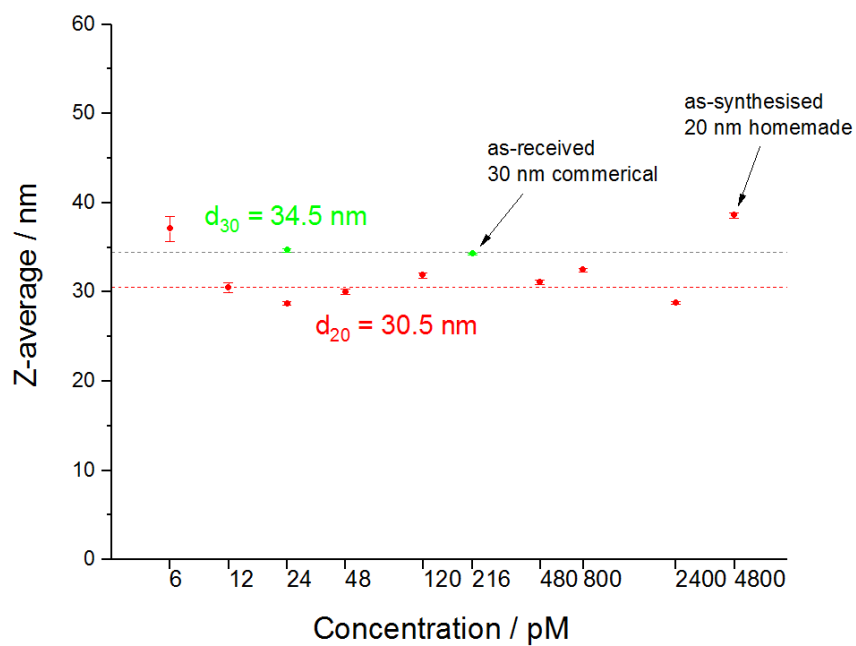


Figure S2. DLS sizing of the '20 nm' (red) and '30 nm' (green) Ag NPs with concentrations 6 to 4800 pM with near no salt presence (< 2 mM citrate).

S3 – Effects of windowing and weighting on the nano-impact sizing results

The measured spike signals need to be processed to reveal the ‘true’ effective diameter distributions by two-fold considerations based on the particulate motion in the dispersion.

First, there is the question of the simultaneous collisions of two or more particles with the electrode and being detected at the same time. To statistically study the spike datasets and answer the question, we define a time window during which only one or zero single nanoparticle can, with 99% confidence, arrive at the electrode surface. In other words, there is a 99% probability of impacts of up to one particle that occur within the time interval. Any two or more spikes detected within this time period are clustered as single features (i.e. multi-collisions of the same particle with the electrode) and their charges are summed. This time window can be quantified by probability theory of a Poisson distribution. Under the assumption of independent impact events, a model of Poisson distribution as follows is provided,

$$P(k = \lambda t) = e^{-\lambda} \frac{\lambda^k}{k!}$$

where P is the probability, k is the number of events in a certain time interval t , and λ is the average occurrence rate of such events.

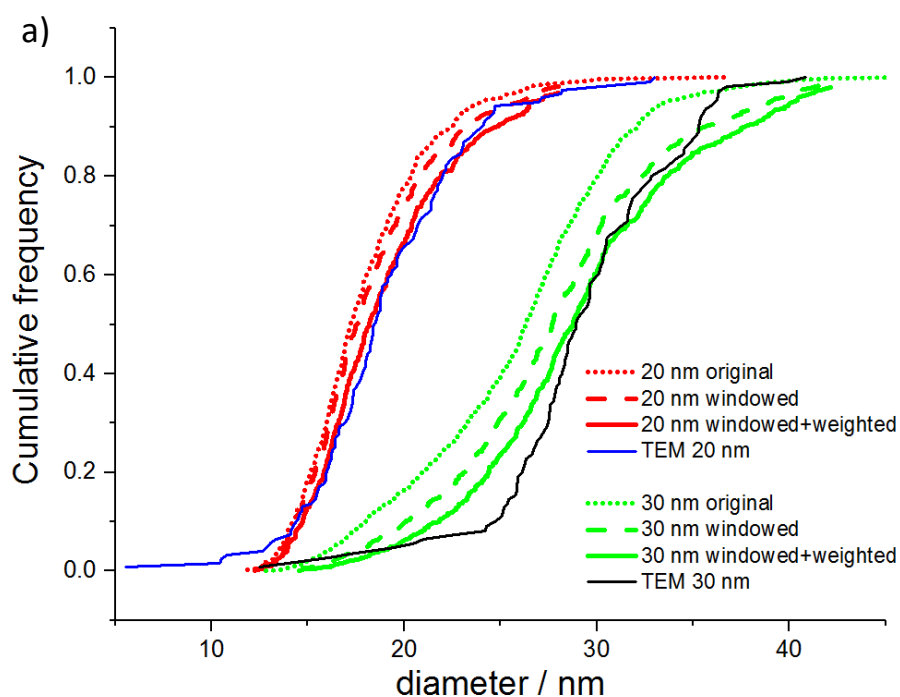
Next, to calculate the time window t , assuming a steady-state diffusion flux of the particles to the microdisc electrode,³

$$J = 4 D c r$$

where J is the steady-state flux (s^{-1}), D and c is the diffusion coefficient ($m^2 s^{-1}$) and particle concentration (m^{-3}) of the NPs respectively, and r is the microelectrode radius (m^{-1}).

Herein, the calculated flux J is the average occurrence rate λ in the Poisson distribution equation. As a result, such time windows are found to be 36 ms for the '30 nm'-diameter particles and 21 ms for the '20 nm' particles.

Second, smaller particles move faster thus having higher probability of colliding with the electrode. Therefore, the windowed diameter distributions are further weighted for diffusion based on the diffusion coefficients of the individual particles. As a result, the Figure S3 shows that the impact frequencies of both samples stay almost unchanged; however, the charges of the larger '30 nm' sample increase to a larger extent as many spikes were observed occurring over twice within the window size of 36 ms due to its high impact frequency. In this way, the windowing effectively combines multiple signals that originate very likely from single impact event and reveals the 'true' sizes of the samples. The origins of multiple signals from a single event likely reflect a particle at the interface moving so as to vary the electron tunnelling distance between the electrode and the nanoparticle.⁴



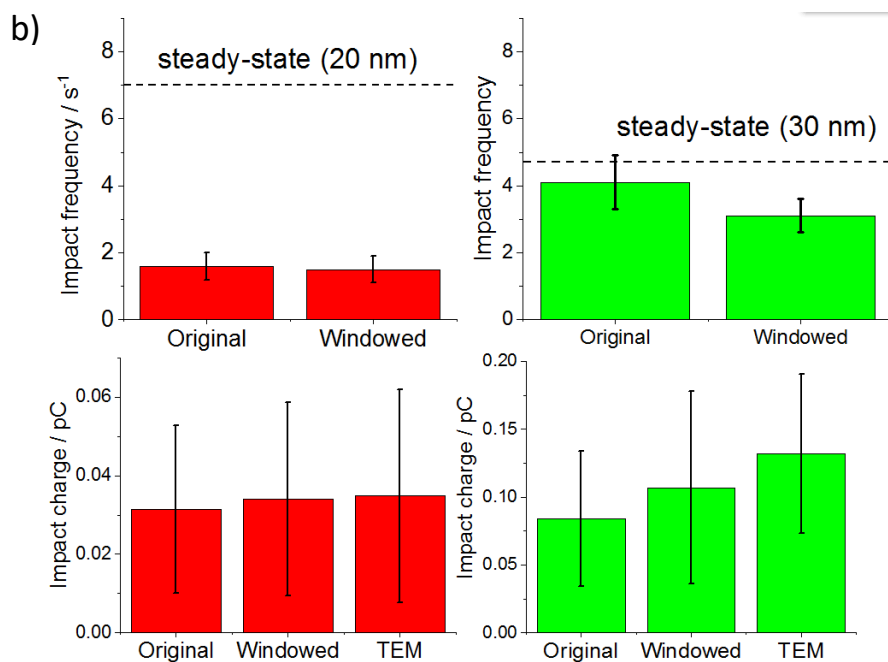


Figure S3. a) Cumulative frequency diameter distribution for nano-impact events of the ‘20 nm’ and ‘30 nm’ silver particles. Red dotted, dashed and solid lines represent the original (or not windowed) data of the ‘20 nm’ silver particles, while the green lines are for the ‘30 nm’ particles. Blue and black solid lines denote TEM sizing curves for the ‘20 and 30 nm’ particles respectively. b) The second group of figures show impact frequencies before and after windowing for the ‘20 nm’ (red) and ‘30 nm’ (green) silver particles, with predicted steady-state frequencies shown as the dotted black lines; and impact charges before and after windowing as compared to the charges derived from TEM results.

References

1. E. Tomaszewska, K. Soliwoda, K. Kadziola, B. Tkacz-Szczesna, G. Celichowski, M. Cichomski, W. Szmaja and J. Grobelny, *Journal of Nanomaterials*, 2013, **2013**, 60.
2. D. Langevin, O. Lozano, A. Salvati, V. Kestens, M. Monopoli, E. Raspaud, S. Mariot, A. Salonen, S. Thomas and M. Driessen, *Nanoimpact*, 2018, **10**, 97-107.
3. R. G. Compton and C. E. Banks, *Understanding voltammetry*, World Scientific, 2011.
4. S. M. Oja, D. A. Robinson, N. J. Vitti, M. A. Edwards, Y. Liu, H. S. White and B. Zhang, *Journal of the American Chemical Society*, 2016, **139**, 708-718.